A Thesis

On

SINGLE PHASE SYNTHESIS OF RUTILE TiO_2 NANOPARTICLES

Submitted in the partial fulfillment of requirement for the award of the degree of

Master of Technology

in

MATERIALS & METALLURGICAL ENGINEERING

by

RAJNI SHARMA

Roll No - 600802017

Under the supervision of

Dr. O.P. PANDEY (Prof. & Head of Dept.) **&** **Dr. B.N. Chaudasama** (Assistant Prof.)

School of Physics & Materials Science

Thapar University

Patiala – 147001

July-2010

Dedicated to my loving Parents

CERTIFICATE

I hereby certify that the work which is being presented in the thesis entitled, ***" Single Phase Synthesis of Rutile TiO_2 Nanoparticles"*** *submitted by Ms. RAJNI SHARMA, Roll No. 600802017 in the partial fulfillment of the requirements for the award of degree of* ***MASTERS OF TECHNOLOGY*** *in* ***"Materials and Metallurgical Engineering"*** *from the* ***School of Physics and Material Science*** *of* ***Thapar University, Patiala****, is an authentic record of my own work carried out under the supervision of Dr. O.P. Pandey and Dr. B.N. Chaudasama and refers other researcher's works which are duty listed in the reference section.*

This is to certify that the above statement made by the candidate is correct and true to the best of my knowledge.

(Prof. O.P. Pandey)
Supervisor
Thapar University, Patiala-147001

(Dr. B.N. Chaudasama)
Supervisor
Thapar University, Patiala-147001

Countersigned by:

Dr. O.P. Pandey,
Professor and Head of the Department,
Thapar University,
Patiala, Punjab.

Dr. R.K. Sharma
Dean Academic Affairs,
Thapar University,
Patiala, Punjab.

ACKNOWLEDGEMENT

At this momentous occasion of binding my thesis I would like to acknowledge the contribution of all those benevolent people. I have been blessed to associate with. Behind every student, there stand a myriad of people whose help and contribution makes things successful. Since such a list can be a prohibitively long, we may be excused for any omissions. My first and foremost offering of thanks goes to the architect who shaped my dreams into reality, my guide and mentor **Dr. O.P. Pandey, Professor and Head, School of Physics and Materials Science** and **Dr. B.N. Chaudasama, Assistant Professor, School of Physics and Materials Science**. Preserverance, exuberance, positive approaches are just some of the traits both imprinted on my personality. Both steered me through their journey through their invaluable advice positive criticism, stimulating discussion and consistent encouragement. Their meticulous attention towards my proceedings, their devoted time and their ideas has enabled me to make the project a success. Their faith in me has always made me more confident. Their blessing always made me optimistic. It had been my privilege to work under their guidance.

My greatest thanks are to **Dr. Kulvir Singh, Associate Professor and PG Incharge, School of Physics and Materials Science** for his encouragement and execution of thesis work. I would also like to thank **Dr. K.K. Raina, Professor and Deputy Director, School Of Physics and Materials Science** for his guidance and encouragement. I am also thankful to **Dr. D.P. Singh, Dr. Puneet Sharma, Dr. S.D. Tiwari** and all the faculty members of School of Physics and Materials Science for their constructive suggestions at different stages of this work. My special thanks to Lab supdt. (SPMS), **Mr. Purshottam**. His assistance and partnership were of great pleasure. His comments and views were very insightful and helpful. I would also like to thank **Mr. Jant Singh** for providing all kind of assistance in PG Lab for creating a healthy research environment.

I would like to convey my sincere gratitude to my friends and colleagues **Poonam Benjwal, Ramkishor, Rashmi, Paramjot, Poonam Sharma** for their support and their timely help and valuable discussions.

I owe my sincere thanks to all the staff members of School of Physics and Materials Science for their support and encouragement. The meaning of my life and work is incomplete without paying regards to my respected parents whose blessings and continuous encouragement have shown me the path to achieve my goals. And above all, I pay my regards to the **Almighty** for his love.

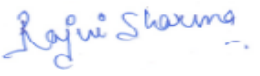

(Rajni Sharma)

Abstract

The hydrolysis method was utilized to synthesis TiO_2 nanoparticles as pure rutile phase and ammonia in acidic medium by adjusting the pH around 10. Nano TiO_2 were prepared from $TiCl_4$ and HPLC grade water as solvent. The synthesized TiO_2 nanoparticles was calcined at 400 ^{0}C, 700 ^{0}C and 900 ^{0}C for 4 hours. Structural, morphological and chemical properties of synthesized TiO_2 nanoparticles were investigated by X-ray diffraction (XRD), Scanning electron microscopy (SEM), Transmission electron microscopy (TEM) & Fourier transform infrared microscopy (FTIR) respectively. The experiment indicates that hydrolysis and drying have important effects on the properties of product. On finding shows the formation of pure rutile phase of nano TiO_2 in basic medium. The calculated particle size of TiO_2 nanoparticles was in the range of 20-30 nm. Also the structural characterization shows the formation of mixed phase (anatase + rutile) of nano TiO_2 particles which indicates the unreacted reaction in acidic medium.

CONTENTS

List of Figures

List of Tables

Chapter-1

Introduction and Review of Literature

INTRODUCTION

1.1 Historical Background of TiO_2

The element Titanium was discovered in 1791 by William Gregor, in England. Gregor spent much of his time studying mineralogy, which led him to his discovery. This happened when he discovered a sample of a black sandy substance in his neighbourhood. He studied this substance and after he was assured that it was a mineral, he called it menachanite. Four years later a man named Martin H. Klaproth, recognized that there was a new chemical element in this mineral, he later named it Titanium after the Titans, which were humongous monsters that ruled the world in Greek mythology. Martin H. Klaproth was not able to make the pure element of titanium however, he was only able to produce TiO_2, or Titanium Dioxide [1].

1.2 Occurrence

Titanium dioxide occurs in nature as well-known minerals rutile, anatase and brookite, and additionally as two high pressure forms, a monoclinic baddeleyite-like form and an orthorhombic α-PbO_2-like form, both found recently at the Ries crater in Bavaria [2,3]. The most common form is rutile, which is also the most stable form. Anatase and brookite both convert to rutile upon heating [4]. Rutile, anatase and brookite all contain six coordinated titanium. Titanium dioxide has eight modifications - in addition to rutile, anatase and brookite there are three metastable forms produced synthetically (monoclinic, tetragonal and orthorhombic), and five high pressure forms. (α-PbO_2-like, baddeleyite-like and cotunnite-like).

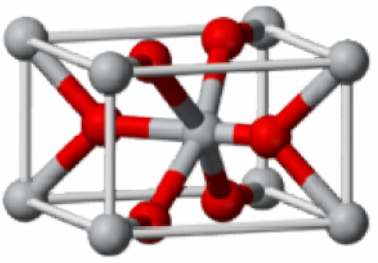

Figure 1.1 Structure of TiO_2 [2]

The naturally occurring oxides can be mined and serve as a source for commercial titanium. The metal can also be mined from the other minerals such as ilmenite or leucoxene ores, or one of the purest forms, rutile beach sand. These ores are the principal raw materials used in the manufacture of titanium dioxide pigment. The first step is to purify the ore, and is basically a

refinement step. Either the sulphate process, which uses sulphuric acid as an extraction agent or the chloride process, which uses chlorine, may achieve this. After purification the powders may be treated (coated) to enhance their performance as pigments [5,6].

1.3 Properties of Titania

Physical and mechanical properties of sintered titania are summarised in table 1.1, while optical properties are shown in table 1.2.

PROPERTY	RANGE
Density	4 g/cm^3
Porosity	0 %
Modulus of Rupture	140 MPa
Compressive Strength	680 MPa
Poisson's Ratio	0.27
Fracture Toughness	3.2 $Mpa.m^{-1/2}$
Shear Modulus	90 GPa
Modulus of Elasticity	230 GPa
Microhardness (HV0.5)	880
Resistivity (25 ^0C)	10^{12} ohm.cm
Resistivity (700 ^0C)	$2.5x10^4$ ohm.cm
Dielectric Constant (1MHz)	85
Dissipation factor (1MHz)	$5x10^{-4}$
Dielectric strength	4 $kVmm^{-1}$
Thermal expansion (RT-1000 ^0C)	$9x10^{-6}$
Thermal Conductivity (25 ^0C)	11.7 WmK^{-1}

Table 1.1 Physical and mechanical properties of Titania [4]

Phase	Refractive Index	Density ($g.cm^{-3}$)	Crystal Structure
Anatase	2.49	3.84	Tetragonal
Rutile	2.91	4.26	Tetragonal

Table 1.2 Optical properties of Titania [4]

1.4 Uses

Titanium dioxide (TiO_2) is a multifaceted compound. It's the stuff that makes toothpaste white and paint opaque. TiO_2 is also a potent photocatalyst that can break down almost any organic compound when exposed to sunlight, and a number of companies are seeking to capitalize on TiO_2's reactivity by developing a wide range of environmentally beneficial products, including self-cleaning fabrics, auto body finishes, and ceramic tiles. Also in development is a paving stone that uses the catalytic properties of TiO_2 to remove nitrogen oxide from the air, breaking it down into more environmentally benign substances that can then be washed away by rainfall. Other experiments with TiO_2 involve removing the ripening hormone ethylene from areas where perishable fruits, vegetables, and cut flowers are stored; stripping organic pollutants such as trichloroethylene and methyl-tert-butyl ether from water; and degrading toxins produced by blue-green algae. It remains to be seen, however, whether the formation of undesirable intermediate products during these processes outweighs the benefits offered by TiO_2's photocatalytic properties [1].

Titanium dioxide is a well-known photocatalyst for water and air treatment as well as for catalytic production of gases. The general scheme for the photocatalytic destruction of organics begins with its excitation by supra band gap photons, and continues through redox reactions where OH radicals, formed on the photocatalyst surface, play a major role. Titanium dioxide is non-toxic and therefore is used in cosmetic products (sunscreens, lipsticks, body powder, soap, pearl essence pigments, tooth pastes) and also in special pharmaceutics. Titanium dioxide is even used in food stuffs, for instance in the wrapping of salami. Small amounts added to cigar tobacco are the cause of the white ash cigar smokers so cherish [1].

1.4.1 As a storage medium

Researchers at the University of Tokyo, Japan have created a 25 terabyte titanium oxide-based disc [7].

1.4.2 Oxygen Sensors

Even in mildly reducing atmospheres Titania tends to lose oxygen and become sub stoichiometric. In this form the material becomes a semiconductor and the electrical resistivity of the material can be correlated to the oxygen content of the atmosphere to which it is exposed. Hence titania can be used to sense the amount of oxygen (or reducing species) present in an atmosphere [3].

1.4.3 Antimicrobial Coatings

The photocatalytic activity of titania results in thin coatings of the material exhibiting self cleaning and disinfecting properties under exposure to UV radiation. These properties make the material a candidate for applications such as medical devices, food preparation surfaces, air conditioning filters, and sanitary ware surfaces [3].

1.5 Applications

Applications for sintered titania are limited by its relatively poor mechanical properties. It does however find a number of electrical uses in sensors and electrocatalysis. By far its most widely used application is as a pigment, where it is used in powder form, exploiting its optical properties [1].

1.5.1 Pigments

Titanium dioxide is the most widely used white pigment because of its brightness and very high refractive index (n = 2.7), in which it is surpassed only by a few other materials. Approximately 4 million tons of pigmentary TiO_2 are consumed annually worldwide. When deposited as a thin film, its refractive index and colour make it an excellent reflective optical coating for dielectric mirrors and some gemstones like "mystic fire topaz". TiO2 is also an effective opacifier in powder form, where it is employed as a pigment to provide whiteness and opacity to products such as paints, coatings, plastics, papers, inks, foods, medicines (i.e. pills and tablets) as well as most toothpastes. Opacity is improved by optimal sizing of the titanium dioxide particles. Titanium dioxide is often used to whiten skimmed milk [8].

In cosmetic and skin care products, titanium dioxide is used as a pigment, sunscreen and a thickener. It is also used as a tattoo pigment and instyptic pencils. Titanium dioxide is produced in varying particle sizes, oil and water dispersable, and with varying coatings for the cosmetic industry. This pigment is used extensively in plastics and other applications for its UV resistant

properties where it acts as a UV absorber dioxide, efficiently transforming destructive UV light energy into heat. In ceramic glazes titanium acts as an opacifier and seeds crystal formation.

Titanium dioxide is found in almost every sunscreen with a physical blocker because of its high refractive index, its strong UV light absorbing capabilities and its resistance to discolouration under ultraviolet light. This advantage enhances its stability and ability to protect the skin from ultraviolet light. Sunscreens designed for infants or people with sensitive skin are often based on titanium dioxide and/or zinc oxide, as these mineral UV blockers are believed to cause less skin irritation than chemical UV absorber ingredients. The titanium dioxide particles used in sunscreens have to be coated with silica or alumina, because titanium dioxide creates radicals in the photocatalytic reaction. These radicals are carcinogenic, and could damage the skin [8].

1.5.2 Photocatalyst

The photocatalytic properties of titanium dioxide were discovered by Akira Fujishima in 1967 [9] and published in 1972 [10]. The process on the surface of the titanium dioxide was called the Honda-Fujishima effect [9]. Titanium dioxide, particularly in the anatase form, is a photocatalyst under ultraviolet (UV) light. Recently it has been found that titanium dioxide, when spiked with nitrogen ions or doped with metal oxide like tungsten trioxide, is also a photocatalyst under either visible or UV light. It can also oxidize oxygen or organic materials directly.

Titanium dioxide is thus added to paints, cements, windows, tiles, or other products for its sterilizing, deodorizing and anti-fouling properties and is used as a hydrolysis catalyst. It is also used in the Graetzel cell, a type of chemical solar cell. A substance that helps bring about a light catalyzed reaction, such as chlorophyll in photosynthesis. Like photosynthesis, the reaction continues throughout the day once begun [1].

Titanium dioxide has potential for use in energy production: as a photocatalyst, it can

- Carry out hydrolysis; i.e., break water into hydrogen and oxygen. Were the hydrogen collected, it could be used as a fuel. The efficiency of this process can be greatly improved by doping the oxide with carbon [11].
- Titanium dioxide can also produce electricity when in nanoparticles form. Research suggests that by using these nanoparticles to form the pixels of a screen, they generate electricity when transparent and under the influence of light. If subjected to electricity on the other hand, the

nanoparticles blacken, forming the basic characteristics of a LCD screen. According to creator Zoran Radivojevic, Nokia has already built a functional 200*200-pixel monochromatic screen, which is energetically self-sufficient.

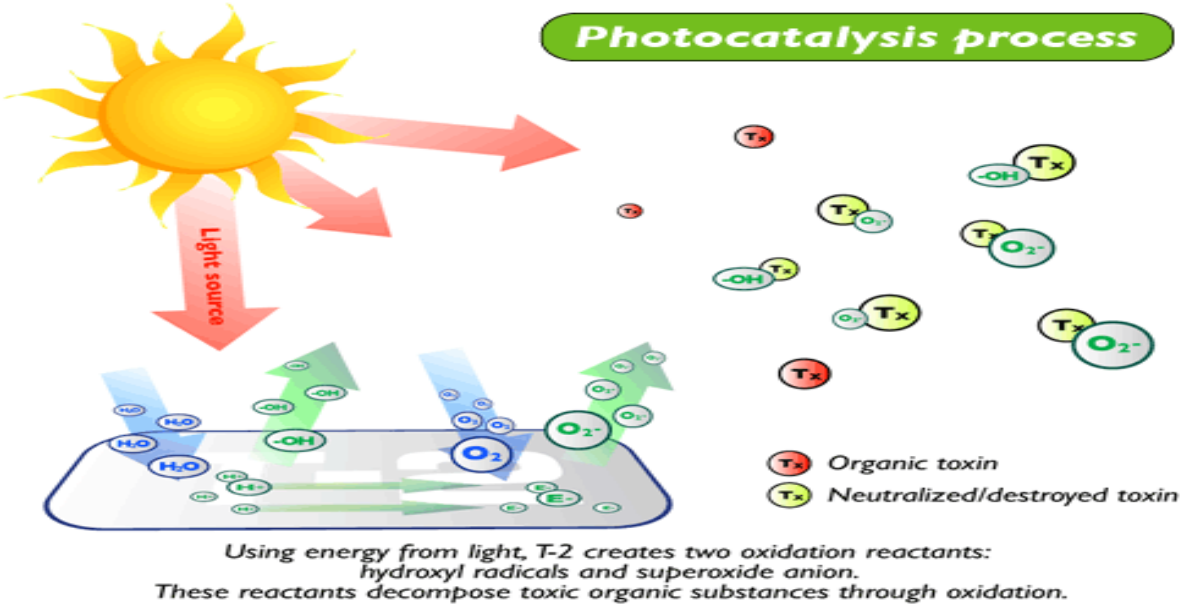

Figure 1.2 Photocatalytic process [1]

In 1995 Fujishima and his group discovered the super hydrophilicity phenomenon for titanium dioxide coated glass exposed to sun light [9]. This resulted in the development of self-cleaning glass and anti-fogging coatings.TiO_2 incorporated into outdoor building materials, such as paving stones in noxer blocks or paints, can substantially reduce concentrations of airborne pollutants such as volatile organic compounds and nitrogen oxides. A photocatalytic cement that uses titanium dioxide as a primary component, produced by Italcementi Group, was included in Time's Top 50 Inventions of 2008 [12]. TiO_2 offers great potential as an industrial technology for detoxification or remediation of waste water due to several factors:-

1. The process occurs under ambient conditions very slowly; direct UV light exposure increases the rate of reaction.
2. The formation of photocyclized intermediate products, unlike direct photolysis techniques, is avoided.
3. Oxidation of the substrates to CO_2 is complete.
4. The photocatalyst is inexpensive and has a high turn over.
5. TiO_2 can be supported on suitable reactor substrates.

1.5.3 Other applications are

- It is also used in resistance-type lambda probes (a type of oxygen sensor).
- Titanium dioxide is what allows osseointegration between an artificial medical implant and bone [13].
- Titanium dioxide in solution or suspension can be used to cleave protein that contains the amino acid proline at the site where proline is present. This breakthrough in cost-effective protein splitting took place at Arizona State University in 2006 [14].
- Titanium dioxide on silica is being developed as a form of odour control in cat litter. The photocatalyst is vastly cheaper than silica beads per usage and effectively eliminates odour for longer.
- Titanium dioxide is also used as a material in the memristor, a new electronic circuit element. It can be employed for solar energy conversion based on dye, polymer, or quantum dot sensitized nanocrystalline TiO_2 solar cells using conjugated polymers as solid electrolytes [15].
- It has also been recently incorporated as a photocatalyst into dental bleaching products. It allows the use of decreased concentrations of hydrogen peroxide in the bleaching agent, thus claimed to achieve similar bleaching effects with fewer side effects (e.g. transient sensitivity, change in tooth surface topography, etc.)
- It is also used by film and television companies as a substitute for snow when filming scenes which require a winter setting.
- Synthetic single crystals and films of TiO_2 are used as a semiconductor [16], and also in Bragg-stack style dielectric mirrors due to the high refractive index of TiO_2 (2.5 – 2.9) [17].

1.6 Health and safety

Titanium dioxide is incompatible with strong oxidizers and strong acids. Violent or incandescent reactions may occur with metals (e.g. aluminium, calcium, magnesium, potassium, sodium, zinc and lithium) [18].

Titanium dioxide dust, when inhaled, has recently been classified by the International Agency for Research on Cancer (IARC) as an IARC Group 2B carcinogen possibly carcinogenic to humans [19]. Many sunscreens use nanoparticle titanium dioxide (along with nanoparticle ZnO) which does get absorbed into the skin. This could cause as of yet unknown health problems [20]. The findings of the IARC are based on the discovery that high concentrations of pigment-grade (powdered) and ultrafine TiO_2 dust caused respiratory tract cancer in rats exposed by inhalation and intratracheal instillation [21]. The series of biological events or steps that produce

the rat lung cancers (e.g. particle deposition, impaired lung clearance, cell injury, fibrosis, mutations and ultimately cancer) have also been seen in people working in dusty environments. Therefore, the observations of cancer in animals were considered, by IARC, as relevant to people doing jobs with exposures to TiO_2 dust. For example, titanium dioxide production workers may be exposed to high dust concentrations during packing, milling, site cleaning and maintenance, if there are insufficient dust control measures in place. However, it should be noted that the human studies conducted so far do not suggest an association between occupational exposure to TiO_2 and an increased risk for cancer. The safety of the use of nanoparticles sized TiO_2, which can penetrate the body and reach internal organs, has been criticized. Studies have also found that TiO_2 nanoparticles cause genetic damage in mice, suggesting that humans may be at risk of cancer or genetic disorders resulting from exposure [21].

1.7 Methods of preparation

There are number of methods with which TiO_2 nanoparticles can be prepared.

1.7.1 With $TiCl_4$ aqueous solution

Pure anatase TiO_2 phase nanocrystallites were synthesized directly from a $TiCl_4$ aqueous solution using citric acid as an additive. On the other hand, hydrothermal autoclaving of the rutile TiO_2 embryos prepared by room temperature peptization of the $TiCl_4$ aqueous solution gave rod like rutile TiO_2 nanocrystallites under neutral conditions [22].

1.7.2 With carbon dioxide

Nanosized titanium dioxide TiO_2 powder was successfully prepared from its precursor titanium (IV) isopropoxide (TTIP) by a system comprising of supercritical fluids micro emulsion and supercritical-drying method, in which TTIP reacted in reversed micelles formed by surfactant Zonyl FSJ employing a supercritical carbon dioxide system [23].

1.7.3 By optimized process

TiO_2 (rutile/anatase) dispersions were prepared in distilled water by treatment with different ultrasound energies and various dispersion stabilizers (1.0% carboxymethyl cellulose, 0.5% hydroxypropyl methyl cellulose K4M, 100% fetal bovine serum, and 2.5% bovine serum albumin. The optimized process for preparation of TiO_2 (rutile/anatase) nanoparticles dispersion is to vibrate the nanoparticles by vortex and disperse them by ultrasonic vibration in distilled water, then to add dispersion stabilizers to the dispersion, and finally to sonicate the nanoparticles

in dispersion. This method is practicable to prepare a stable dispersion of TiO_2 (rutile/anatase) nanoparticles for at least 120 hr [24].

1.7.4 By spray deposition

Low temperature(180–240 ^{0}C) synthesis of nanocrystalline titanium dioxide (TiO_2) by surfactant-free solvothermal route is investigated. Titanium iso-propoxide is used as the precursor and toluene as the solvent. The films deposited by spray deposition method using these nanoparticles show the crystalline and porous nature of the films. The present method of deposition also avoids the post-treatment (sintering) of the films. The nanoparticles thus prepared and the films can be used for gas sensing and biological applications and also as photo-electrodes for dye-sensitized solar cells [25].

1.8 REVIEW OF LITERATURE

1.8.1 Literature survey

Hengbo Yin et al. [2001] studied the synthesis of phase- pure nano-particulate anatase and rutile TiO_2 using $TiCl_4$ aqueous solutions. Here phase- pure anatase TiO_2 nanocrystallites ranging from 2 to 10 nm in size were synthesized directly from a $TiCl_4$ aqueous solution using citric acid as an additive. Citric acid was found to play a decisive role in stabilizing the $TiCl_4$ aqueous solution, leading to the selective formation to the anatase TiO_2 nanocrystallites in hydrothermal autoclaving. On the other hand, hydrothermal autoclaving of the rutile TiO_2 embryos prepared by room temperature peptization of the $TiCl_4$ aqueous solution give rod-like rutile TiO_2 nanocrystallites under neutral conditions. The presence of KCl or NaCl enhanced the crystal growth of the rutile embryos in the hydrothermal process [22].

In this study they have concluded that Nano-particulate rutile TiO_2 nanocrystallites with rod-like shapes were prepared by hydrothermal treatment at high temperature of the rutile embryos prepared by hydrolysis of $TiCl_4$ aqueous solution at low temperature. Water as a neutral reaction medium was beneficial to the formation of the well-particulate rutile nanocrystallites. The presence of NaCl and KCl in the hydrothermal processing of rutile embryos enhanced the crystal growth via coalescence of the embryos.

Chie- I Wu et al. [2008] studied that Nano-sized titanium dioxide TiO_2 powder was successfully prepared from its precursor titanium (IV) isopropoxide (TTIP) by a system comprising of

supercritical fluids microemulsion and supercritical-drying method, in which TTIP reacted in reversed micelles formed by surfactant Zonyl FSJ employing a supercritical carbon dioxide system. The milky white product, collected from the bottom of the pressure cell turned into sol–gel after sitting in the air for 5 days. Amorphous TiO_2 particles with particles size 2–7 nm can be obtained from the sol–gel by the supercritical-drying method. The amorphous TiO_2 particles were converted to anatase phase by calcining at 500 ^{0}C [23]**.**

Yadong Yao et al. [2009] reported that Titanium dioxide (TiO_2) porous ceramic pellets with three dimension nano-structure were prepared using nano TiO_2 powder. The TiO_2 porous ceramic pellets were composed of TiO_2 nanoparticles with 14–16 nm in diameter and had porosity of 74.85%. The mean pore size of the TiO_2 porous ceramic pellets was 20.73 nm and the main pore size ranged from 3 to 16 nm. The mass loss of the TiO_2 ceramic pellets was less than 5% after 20 d immersion in water. The antibacterial properties of the TiO_2 pellets were studied. The sterilization rate of *Colibacillus* (hospital polluted water with bacterium) can reach 99% after 3 h photocatalytic process and these TiO_2 pellets are easy to be re-activated and cyclically be used [26].

Zhang et al. [2005] studied that TiO_2 nanoparticles were introduced into High-impact polystyrene (HIPS) in the form of master batch where TiO_2 was pre-dispersed in HIPS by melt compounding [27]. Energy dispersive X-ray spectrometer (EDS) composition distribution maps indicate that TiO_2 nanoparticles are dispersed randomly in the nanocomposites comprising low TiO_2 content (≤2wt.%), while the dispersion is inferior at high TiO_2 content. The variation in the dispersion behavior influences the mechanical properties of nanocomposites. Significantly, the surface of nanocomposites shows a strong absorption of UV light in the wavelength range of 250□400 nm, an increase in the TiO_2 content of nanocomposites raises the absorbance in the region. HIPS/TiO_2 nanocomposites have a satisfactory antibacterial effect on *Escherichia coli (E. coli) and Staphylococcus aureus (S. aureus)* [27].

Xu Wei-guo et al. [2004] studied that TiO_2 nanometer thin film with photocatalytic antibacterial activity were prepared by the sol gel method on fused quartz and soda lime glass precoated with a SiO_2 layer. The thin films were characterized by X-ray photoelectron spectroscopy, scanning electron microscopy and X-ray diffraction. The results show that sodium and calcium diffusion into nascent $Ti0_2$ film is effectively retarded by the SiO_2 layer precoated on the soda lime glass. The antibacterial activity of the films was determined. The crystalline of TiO_2 nanometer thin film has an important effects on the antibacterial activity of the film [28].

Vilas S. Desai et al. [2009] studied that the process of heterogeneous photocatalysis (HP) using TiO_2 photocatalysts. This study reports the synthesis of a visible light responsive nanosized TiO_2 photocatalyst by a modified sol-gel process. The synthesized TiO_2 photocatalyst exhibits photocatalytic activity against some common pathogenic microorganisms such as *Escherichia coli, Pseudomonas aeruginosa, Klebsiella pneumonia* and *Staphylococcus aureus* under visible light illumination. TiO_2 is known to exhibit photocatalytic activity under UV light irradiation, the results obtained in the study using solar irradiation are very promising and enables the use of cheaply available solar energy for the process of photocatalysis [29].

In this study they have concluded that TiO_2 synthesized by sol-gel method exhibits bactericidal activity when irradiated with sunlight against the common human pathogens tested. This opens up newer avenues for the development of solar assisted alternative technologies for disinfection of water bodies contaminated with pathogenic organisms.

Guifen Fu et al. [2005] studied a sol-gel chemistry approach was used to fabricate nanoparticles of TiO_2 in its anatase form. The particle size is shown to be sensitive to the use of $HClO_4$ or HNO_3 as acid catalyst. The gold-capped TiO_2 nanocomposites were processed by the reduction of gold on the surface of the TiO_2 nanoparticles via a chemical reduction or a photoreduction method. Different percentages of vanadium-doped TiO_2 nanoparticles, which extended the TiO_2 absorption wavelength from the ultraviolet to the visible region, were successfully prepared. The TiO_2 nanocomposite coatings have been applied on glass slide substrates. The antibacterial activity of TiO_2 nanocomposites was investigated qualitatively and quantitatively. Two types of bacteria, *Escherichia coli (DH 5R) and Bacillus megaterium (QM B1551),* were used during the experiments. Good inhibition results were observed and demonstrated visually. The quantitative examination of bacterial activity for *E. coli* was estimated by the survival ratio as calculated from the number of viable cells, which form colonies on the nutrient agar plates [30].

Huijun Zhang et al. [2006] studied the antibacterial properties of nanometer TiO_2 thin films, nanometer Fe^{3+}-TiO_2 films have been prepared on glass by RF magnetron co-sputtering method. The influence of Fe element and calcination temperature on the films structure was investigated. The principle of substitution impurity to improve the activity was discussed. The bactericidal activity for the bacteria cells was estimated by relative number of bacteria survived calculated from the number of viable cells which from colonies on the nutrient agar plates. The crystallite size of the anatase phase increases with increasing calcinations temperature. The nanometer Fe^{3+} -

TiO_2 thin films exhibited a high antibacterial activity, which was enhanced with the increase of temperature of thermal treatment and formation of anatase crystalline structure [31].

Iram B. Ditta et al. [2008] studied that TiO_2-coated surfaces are increasingly studied for their ability to inactivate microorganisms. The activity of glass coated with thin films of TiO_2, CuO and hybrid CuO/ TiO_2 prepared by atmospheric Chemical Vapour Deposition and TiO_2 prepared by a sol–gel process was investigated using the inactivation of bacteriophage T4 as a model for inactivation of viruses. The chemical oxidising activity was also determined by measuring stearic acid oxidation. The results showed that the rate of inactivation of bacteriophage T4 increased with increasing chemical oxidising activity with the maximum rate obtained on highly active sol–gel preparations. However, these were delicate and easily damaged unlike the Ap-CVD coatings. Inactivation rates were highest on CuO and CuO/TiO_2 which had the lowest chemical oxidising activities. The inactivation of T4 was higher than that of Escherichia coli on low activity surfaces. The combination of photocatalysis and toxicity of copper acted synergistically to inactivate bacteriophage T4 and retained some self-cleaning activity. The presence of phosphate ions slowed inactivation but NaCl had no effect. The results show that TiO_2/CuO coated surfaces are highly antiviral and may have applications in the food and health care industries [32].

S.Q Sun et al. [2008] studied a liquid phase deposition (LPD) method that has been devised for the deposition of Ag–TiO_2 thin films on ceramic tiles with glazed surface at a low temperature. The Ag–TiO_2 thin films obtained were well-adhered, homogenous and coloured by interference of reflected light. From these analyses, it was found that silver ions were trapped in TiO_2 matrix and their reduction could be achieved at 600 ^{0}C annealing temperature. The antibacterial activity against *S. aureus* and *E. coli* has been studied applying the so called antibacterial-drop test. The Ag–TiO_2 thin films exhibited a high antibacterial activity. The releasing rate of silver ions from the Ag–TiO_2 film was 0118 μg/ml during 192 hrs. The antibacterial effect of Ag–TiO_2 thin film before and after aging in a weathering chamber for 48 h was compared and the results show that the antibacterial activity is not compromised after weathering [33].

Huanjun Zhang et al. [2009] studied the antimicrobial properties of Ag-based materials have been actively investigated recently. In such materials, control of the size of the Ag particles is critical to their bactericidal performance. Anovel one-pot sol-gel scheme is described here. It incorporates room temperature ionic liquids (RTILs) to synthesize Ag/TiO_2 nanocomposite powders. The presence of RTILs is indispensable to the control of the size of the Ag particles. Highly dispersed, metallic Ag nanoclusters are formed on the TiO_2 nanoparticles surface after

calcination of the gel. The average cluster size of Ag can be controlled to be below 5 nm with high Ag loading (7.4 wt%). Antibacterial tests using 7.4wt% Ag/TiO_2 on 105 CFU/ml *Escherichia coli (E. coli)* strains incubated on Luria-Bertani (LB)/agar plates show that bacterial growth was inhibited by 98.8% at an Ag concentration of 1.2 μg/ml. Complete inhibition was achieved at 2.4 μg (Ag)/ml. At this concentration, a 3.9wt% Ag/TiO_2 sample, with a smaller Ag cluster size (<3 nm), completely inhibited bacterial growth in a more populated E. coli community (□3 × 106 CFU/m;). In fact, 1.6 μg/ml Ag suppressed bacterial growth by 99.9% with 3.9wt% Ag/TiO_2. Both the small Ag cluster size and the unique structure of TiO_2 nanoparticles supporting highly dispersed Ag clusters are identified to be the sources of a superior bactericidal performance of the RTILs derived Ag/TiO_2 [34].

San-Xiang Tan et al. [2009] studied the hydrothermal method was used to prepare TiO_2@C core–shell composite using TiO_2 as core and sucrose as carbon source. TiO_2@C served as a support for the immobilization of Ag by impregnation in silver nitrate aqueous solution. The antibacterial properties of the TiO_2@C/Ag core–shell composite against *Escherichia coli (E. coli)* and *Staphylococcus aureus (S. aureus)* were examined by the viable cell counting method. The results indicate that silver supported on the surface of TiO_2@C shows excellent antibacterial activity [35].

Rahmani et al. [2009] studied the photocatalytic disinfection of *Coliform* bacteria as water microbial pollution index using TiO_2 and a low pressure UV lamp in a batch reactor. The polluted water was prepared by adding a colony of *Coliform* in raw water and in separate stages was contacted with UV, TiO_2 and combination of them and various parameters such as contact time, pH and amount of TiO_2 were studied in terms of their effect on reaction progress. The results showed that in simultaneous presence of both UV ray and TiO_2, there was the most effective disinfection of *Coliform*. This study showed that 100% of *Coliform* was killed by irradiation or 60-75 min. in the presence of 0.8 gr l-1 TiO_2 in pH=7.0. Based on the results, UV/TiO_2 process may be effectively applied for disinfection of polluted water and can be suggested as a effective purifying method for water disinfection [36].

Tiangyong Zhang et al. [2009] studied the photocatalytic activity of La and Y when co-doped nano TiO_2 by sol-gel method, and characterized by X-ray diffraction (XRD), specific surface area (BET), scanning electron microscope (SEM) and high resolution transmission electron microscopy (HRTEM). The photocatalytic activity of the $La\text{-}Y/TiO_2$ was evaluated by the degradation of methylene blue (MB) under UV light. Parameters effecting photocatalytic process

such as La and Y doping concentration, calcination temperature, the dosage of catalyst and the pH of MB solution were investigated. The co-doped TiO_2 catalyst showed obviously higher photocatalytic activity for the degradation of methylene blue (MB). The presence of La and Y ions in the TiO_2 particles would prevent the recombination of the electron-hole on the surface of TiO_2 effectively [37].

Shifu chen et al. [2009] studied that TiN/TiO_2 nanoparticle photocatalyst was prepared by ball milling of TiO_2 in H_2O solution doped with TiN. The photocatalyst was characterized by UV–Vis diffuse reflection spectroscopy, X-ray powder diffraction (XRD), and X-ray photoelectron spectroscopy (XPS).Based on the results of the characterization, the mechanism of the increase in photocatalytic activity was investigated. The results show that when the amount of doped TiN is 0.15 wt%, the photocatalytic activity of the TiN/TiO_2 is at its peak. Compared with TiO_2, the photo absorption wavelength range of the TiN/ TiO_2 photocatalyst red-shifts about 30 nm, and the photoabsorption intensity increases as well. The photocatalytic activities of the photocatalyst are higher than that of TiO_2 under UV and visible light irradiation. The increase of surface Ti^{3+} reactive center and the extension of the photoabsorption wavelength are the main factors for the increase in the photocatalytic activity of the TiN/TiO_2. Doped TiN neither changes the TiO_2 crystal phase nor creates new crystal phase by ball milling [38].

They concluded that the photocatalyst TiN/TiO_2 is prepared by ball milling of TiO_2 in H_2O solution doped with TiN. Compared with TiO_2, the photoabsorption wavelength range of the photocatalyst is extended, and the photoabsorption intensity is increased as well. The photocatalytic activity of the TiN/TiO_2 is superior to that of TiO_2 under the UV and visible range of irradiation.

P. Hajkov et al. [2009] studied the photocatalytic activity of silver treated TiO_2 films. The TiO_2 films were deposited on glass substrates by plasma enhanced chemical vapour deposition (PECVD) in a vacuum reactor with radio frequency (RF) low temperature plasma discharge in the mixture of oxygen and titanium isopropoxide vapours (TTIP). The depositions were performed under different deposition conditions. Subsequently, the surface of TiO_2 films was modified by deposition of silver nanoparticles. Photocatalytic activity of both silver modified and unmodified TiO_2 films was determined by decomposition of the model organic matter (acid orange 7). Selected TiO_2 samples were used for tests of antibacterial activity. These tests were performed on Gram-negative bacteria *Escherichia coli*. The results clearly proved that presence

of silver clusters resulted in enhancement of the photocatalytic activity, which was up to four times higher than that for pure TiO_2 films [39].

In this they concluded that Modified TiO_2/PECVD films with high photocatalytic and antimicrobial activity were prepared. Incorporation of silver nanoparticles on the film surface contributes to significant enhancement of the film activity. This effect was observed also on films deposited at nearly room temperature (40 ^{0}C) with very low initial photochemical activity. This effect offers perspective of deposition of antimicrobial active films on heat sensitive substrates.

Beata Tryba et al. [2008] reported that the modification of TiO_2 by doping it with carbon and iron residue can give enhanced photoactivity of TiO_2. Iron adsorbed on the surface of TiO_2 can be an electron or hole scavenger and result in the improvement of the separation of free carriers. The presence of carbon can increase the concentration of organic pollutants on the surface of TiO_2 facilitating the contact of the reactive species with the organic molecules. Carbon-doped TiO_2 can extend the absorption of the light to the visible region and makes the photocatalysts active under visible-light irradiation. It was proved that TiO_2 modified by carbon and iron can work in both photocatalysis and photo-Fenton processes, when H_2O_2 is used, enhancing markedly the rate of the organic compounds decomposition such as phenol, humic acids and dyes. The photocatalytic decomposition of organic compounds on TiO_2 modified by iron and carbon is going by the complex reactions of iron with the intermediates, which significantly accelerates the process of their decomposition. The presence of carbon in such photocatalyst retards the inconvenient reaction of OH radicals scavenging by H_2O_2, which occurs when Fe-TiO_2 photocatalyst is used [40].

They concluded that Modification of TiO_2 by carbon can enhance its photocatalytic activity doped C can extend the light absorption to the visible range and give photocatalytic activity under visible light by the narrowing of the band gap.

E.D. Jeong et al. [2008] studied the visible light photodecomposition activity of gaseous iso-propyl alcohol over Cr and Fe codoped TiO_2 nanoparticles. Doped TiO_2 nanoparticles were synthesized hydrothermally and codopant effects are investigated. Cr and Fe co-doped TiO_2 nanoparticles exhibited two times higher photocatalytic activity for the photodecomposition of gaseous isopropyl alcohol than the individually (Cr/Fe) doped TiO_2 nanoparticles under visible light irradiation ($\lambda > 420$ nm). The activity is mainly correlated to the larger absorption around 496 nm and 563 nm wavelengths by co-doped TiO_2 nanoparticles than Fe doped TiO_2 nanoparticles which possibly absorb $\lambda < 496$ nm [41].

Chapter-2

Experimental Methods

2.1 Synthesis

2.1.1 Materials

Titanium tetrachloride ($TiCl_4$) of Mw =189.71 g/mol, AR grade was purchased from S. D. fine Chemicals Ltd. Aqueous solution were prepared in High performance liquid chromatography (HPLC) grade water (H_2O) of Mw =18.02 g/mol, which was procured from Merck. Ethanol (C_2H_5OH) of Mw = 46.06 was also purchased from Merck. Ammonia (NH_3) of Mw = 17.0385 g/mol and Acetone ($(CH_3)_2CO$) of Mw = 58.08 g/mol were purchased from S. D. fine Chemicals Ltd. All the components are reagent grade and used without further purification.

2.1.2 Synthesis of TiO_2 nanoparticles by hydrolysis of $TiCl_4$

Glasswares (three necks round bottom flask, measuring cylinder, beaker) were first cleaned and rinse with distilled water and acetone and dried in vaccum oven. All the materials and the solvents were weighted with the help of electronic weighing balance and mixed in round bottom flask. A 250 ml three neck flask charged with 200 ml of ice cold water of HPLC grade was added with 10 ml of titanium tetrachloride in a dropwise manner. Then stir it for 30 min until the white fog dissappeared . After that place it on the heating mantle and the reaction was refluxed at 50 ^{0}C for 4 hr. There appeared white precipitate in less than 10 min for refluxing.

Figure 2.1 Experimental set up for the sample preparation

Then centrifuge the precipitates at 6000 rpm and give 4-5 washings with the HPLC grade water. Then filtered the precipitates and heated it in oven at 80 ^{0}C. Then the precipitate was grinded and separate them into three parts i.e. one at room temperature and other two were calcined at different temperatures i.e. at 400 ^{0}C and at 700 ^{0}C for 4 hr. Then these samples were characterized by various experimental techniques.

Whole experiment can be summarised as follows

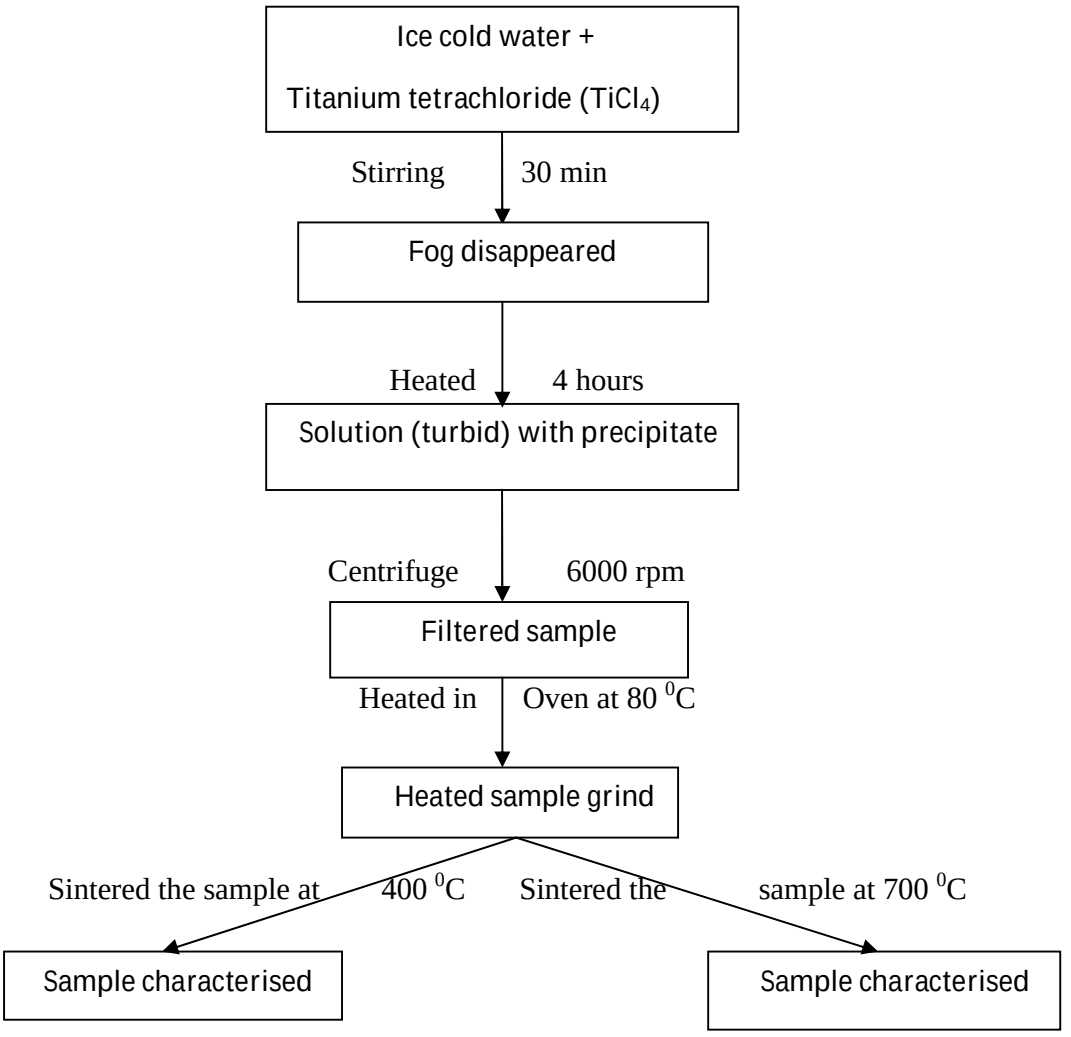

During the filtration, solution was washed by HPLC water many times to avoid the impurities. After filtration, filtered sample was heated at 80 ^{0}C in oven for some time. Heated sample was grinded and sintered at different temperature for 4 hrs (400 ^{0}C, 700 ^{0}C) and characterized under many techniques (like XRD, SEM, TEM, FTIR etc.)

2.1.3 Synthesis of TiO_2 nanoparticles on adding ammonia

A stoichiometric amount of aqueous ammonia with the concentration of 6 ml was dropped into the solution under vigorous stirring and the white precipitate was filtered and washed in the same way.

Whole experiment was summarized as follows

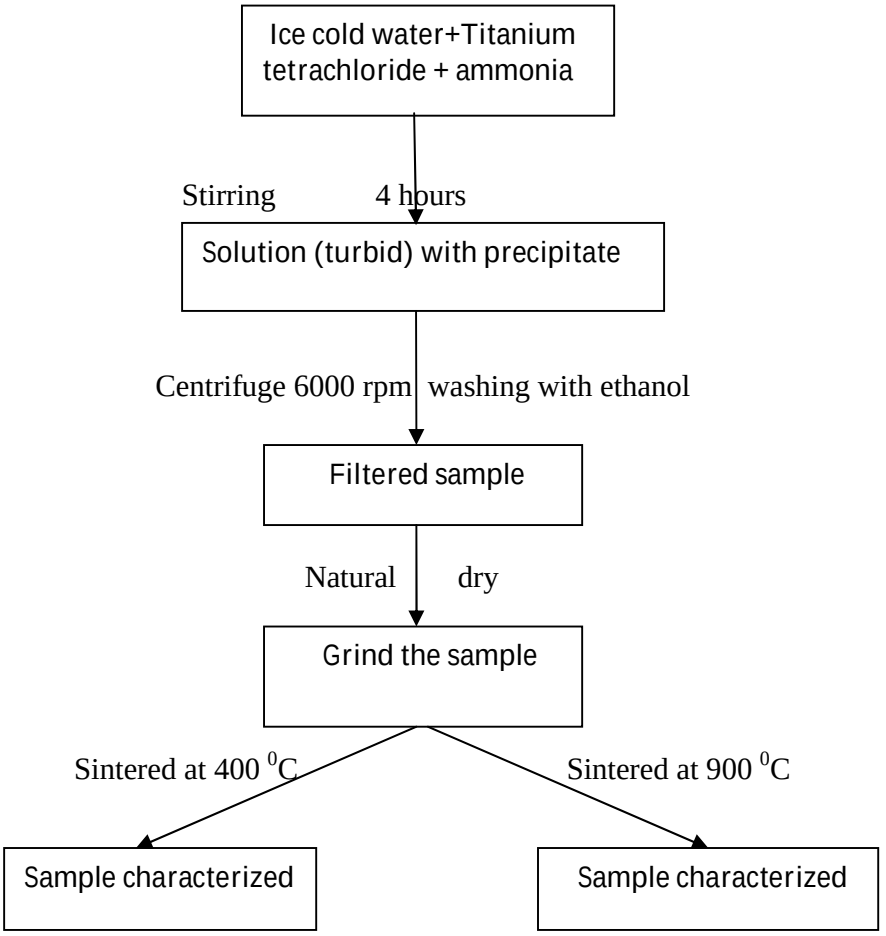

Here during the filtration, solution was washed by ethanol many times to avoid the impurities. After filtration, filtered sample was dried naturally. The sample was grinded and sintered at different temperature for 4 hrs (400 ^{0}C, 900 ^{0}C) and characterized under different number of techniques. (like XRD, SEM, TEM, FTIR etc)

2.2 Characterization Techniques

2.2.1 X-Ray Diffraction (XRD)

X-ray diffraction (XRD) is a versatile, non-destructive technique used for qualitative and quantitative analysis of crystalline materials. This experimental technique has been used to determine the overall structure of solids, including lattice constants, identification of unknown materials, orientation of single crystals, stress, texture, particle size etc. In this study a powder diffraction system with Cu-Kα source (λ=1.54056 A^0) was used. The x-ray scans were performed between 2θ values of 20^0 and 80^0 with a typical step size of about 0.1^0.

2.2.1(a) Generation of X -ray

X-rays are short-wavelength, high energy electromagnetic radiation, having the properties of both waves and particles. X-rays are produced whenever high energy electrons strike with metal target. Any X-ray tube must contain (a) a source of electron (b) a high accelerating voltage (c) a metal target. All X-ray tubes contain two electrodes, an anode (the metal target) usually maintained, at ground potential, and a cathode maintained, at negative potential (normally of order of 30KV to 50KV) for the diffraction work. Interaction that occur between the beam (i.e. electron) and target will result in a loss of energy. A continuous spectrum is formed when the high energy electrons are slowed down rapidly by multiple collisions with the anode material, which give rise to white radiation, or so called Bremsstrahlung.

The continuous spectrum is formed due to rapid deceleration of the electrons hitting the target, as mentioned above, but not every electron decelerates in the same way, some stop in one impact and release all their energy at once, while other deflect this way and that when they encounter atoms of the target, successively losing fractions of their total kinetic energy until is all spent. Those electrons which are stopped in one impact produce photons of maximum energy (wavelength) equal to the energy loss.

2.2.1(b) Bragg's Law

Since atoms are arranged periodically in a lattice, x-rays scattered from a crystalline solid can constructively interfere, producing a diffracted beam through these atoms as shown in figure 2.2. In 1912, W. L. Bragg recognized a predictable relationship among several factors. These factors are combined in Bragg's law:

$$n\lambda = 2d \sin\theta$$

Here, n is an integer,

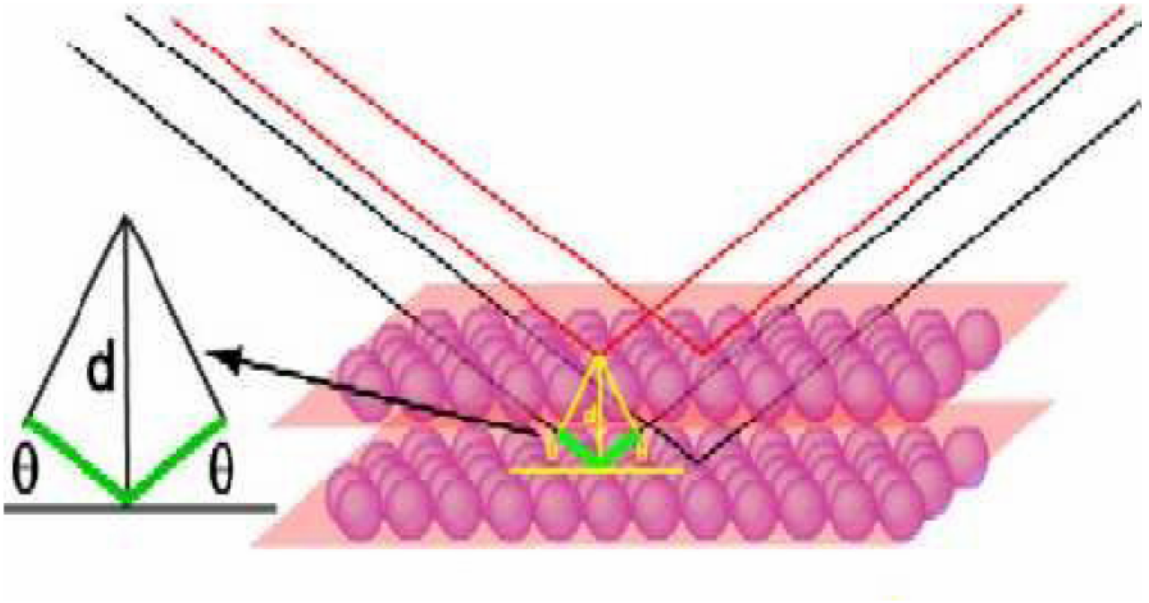

Figure 2.2 Bragg's diffraction condition.

λ is the wavelength of the incident X-ray, d is the distance between set of parallel atomic planes in a mineral (the interatomic spacing) which we call the d-spacing and measure in angstroms and θ is the diffraction angle.

2.2.1(c) Crystallite size measurement : Scherrer's formula

Phase identification using x-ray diffraction depends on the positions of the peaks in a diffraction profile as well as the relative intensities of these peaks to some extent. Another aspect of the diffraction from material is the importance to consider how diffraction peaks are changed by the presence of various types of defects such as small number of dislocations in crystals with dimensions of millimetres. Small size of grain size can be considered as another kind of defect and can change diffraction peak widths. Very small crystals cause peak broadening. The crystallite size is easily calculated as a function of peak width (specified as the full-width at half maximum peak intensity (FWHM)), peak position and wavelength. Scherrer's formula is given as

$$D = 0.9\lambda / B \cos\theta$$

2.2.2 Scanning Electron Microscopy (SEM)

Scanning electron microscope (SEM) is basically a type of electron microscope that images the sample surface by scanning it with a high-energy beam of electrons in a raster scan pattern. The experimental setup is shown in figure 2.3. The electrons interact with the atoms that make up the sample producing signals that contain information about the sample's surface topography, composition and other properties such as electrical conductivity. SEM is used for various purposes like

- Topographic studies and microstructure analysis.
- Elemental analysis (if equipped with appropriate detector (energy/wavelength dispersive x-rays)).
- Chemical composition and elemental mapping.

In SEM, Primary electrons are thermonically or field emitted by a cathode filament (W or LaB) or a filled emission gun (W-tip) and after that accelerated with high energy typically 1-30 KeV. The electron beam is steered with scanning coils over the area of the interest. Upon interaction with material, the primary electrons decelerate as well as losing his energy, transfer it inelastically to other atomic electron and to the lattice.

Figure 2.3 Image of SEM

Due to continuous scattering events the primary beam spread up with different energies depending on source origin as the interaction volume with the various electrons emitted and their respective energy. Secondary electrons (1-50eV) are mostly used for the imaging the topography and to reproduce the surface. High energy elastically backscattered electrons depends on the atomic number (Z) of the element, which is useful to obtain Z-constant. X-ray characteristic can

be used to qualitatively and quantitatively analyze the elemental composition and distribution in the sample as shown in figure 2.4.

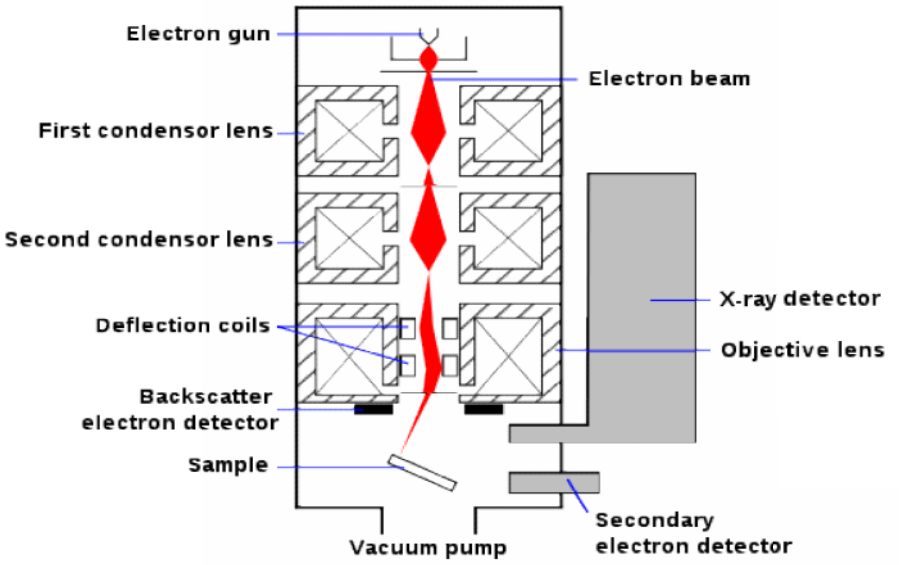

Figure 2.4 Schematic illustration of the SEM

2.2.2(a) SEM setup

The experimental setup consists of an electron gun, column, scanning system, substrate chamber, and detectors.

Electron gun

It is based on the thermal emission. The electron source is commonly a tungsten (W) or lanthanum hexaboride (LaB_6) tip. Electrons are emitted during heating.

Column

The column consists of two electromagnetic lenses acting on the electron beam. The first lens, the condenser lens produces most of the beam demagnification, while the second, objective lens focuses the beam onto the sample. In column, a beam shaper called stigmator, the stigmator can create a magnetic field around the beam to restore it in a circular cross section.

Scanning system

To get image on the display the beam should be scanned over the specimen information from any point on the sample can then reproduced in the same relative position on the display.

Substrate chamber

The substrate holder depends on the different size and shape of the sample. The sample can be moved in three dimensions, as well as rotated and titled.

Detector

The most detector types used for secondary electrons are the scintillation detector. It can also be used for primary electrons.

X-ray detector

Spectrometers for detection and analysis of X-rays are based on either of two principles.

- Wavelength dispersive X-ray (WDX); determines the wavelength of the X-rays.
- Energy dispersive X-ray (EDX); determine the energy of the X-rays.

2.2.3 Fourier Transform Infrared Spectroscopy (FTIR)

FT-IR stands for Fourier Transform Infrared, the preferred method of infrared spectroscopy. The prepared samples were characteried by FTIR spectroscopy. The experimental setup is shown in figure 2.5. In infrared spectroscopy, IR radiation is passed through a sample. Some of the infrared radiation is absorbed by the sample and some of it is passed through (transmitted). The resulting spectrum represents the molecular absorption and transmission, gives information of type of bonding in the sample.

Figure 2.5 Fourier transforms infrared (FTIR) spectrometry

This makes infrared spectroscopy useful for several types of analysis.

• FTIR can identify unknown materials
• FTIR can determine the quality or consistency of a sample
• FTIR can determine the amount of components in a mixture.

The original infrared instruments were of dispersive type. These instruments separated the individual frequencies of energy emitted from the infrared source. This was accomplished by the use of a prism or grating. A grating is a more modern dispersive element which better separates the frequencies of infrared energy. The detector measures the amount of energy at each frequency which has passed through the sample. This results in a spectrum which is a plot of intensity vs. frequency.

Fourier Transform Infrared (FT-IR) spectrometry was developed in order to overcome the limitations encountered with dispersive instruments. The main difficulty was the slow scanning process. A method for measuring all of the infrared frequencies simultaneously, rather than individually, was needed. A solution was developed which employed a very simple optical device called an interferometer. The interferometer produces a unique type of signal which has all of the infrared frequencies “encoded” into it. The signal can be measured very quickly, usually in the order of one second. Thus the time element per sample is reduced to a matter of a few seconds rather than several minutes.

2.2.4 Transmission Electron Microscopy (TEM)

TEM is a microscopy technique whereby a beam of electrons is transmitted through an ultra thin specimen, interacting with the specimen as it passes through as shown in figure 2.6. An image is formed from the interaction of the electrons transmitted through the specimen; the image is magnified and focused onto an imaging device, such as a fluorescent screen, on a layer of photographic film, or to be detected by a sensor such as a CCD camera. TEMs are capable of imaging at a significantly higher resolution than light microscopes, owing to the small de Broglie wavelength of electrons. This enables the instrument's user to examine fine detail even as small as a single column of atoms, which is tens of thousands times smaller than the smallest resolvable object in a light microscope. TEM forms a major analysis method in a range of scientific fields, in both physical and biological sciences. TEMs find application in cancer research, virology, materials science as well as pollution and semiconductor research.

At smaller magnifications TEM image contrast is due to absorption of electrons in the material, due to the thickness and composition of the material. At higher magnifications complex wave interactions modulate the intensity of the image, requiring expert analysis of observed images. Alternate modes of use allow for the TEM to observe modulations in chemical identity, crystal orientation, electronic structure and sample induced electron phase shift as well as the regular absorption based imaging.

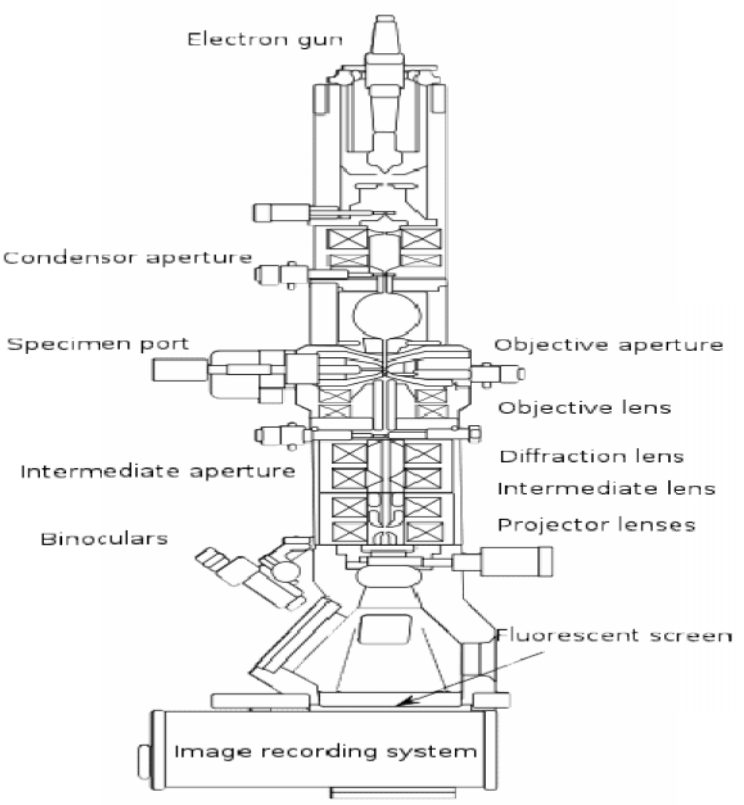

Figure 2.6 Schematic representation of TEM

Chapter-3

Results and Discussions

RESULTS AND DISCUSSIONS

3.1 Synthesis

Aqueous solution of $TiCl_4$ is hydrolyzed by heating at 50 ^{0}C or refluxing under vigorous stirring to produce white precipitate. The XRD spectra show that the precipitate produced by heating at 50 ^{0}C is rutile and by refluxing is a mixture of anatase and rutile. The formation of anatase is attributed to the low pH of solution. The size of the precipitate particles is big and the specific surface area of dried powder is small. When ammonia is added in $TiCl_4$ solution, a great amount of precipitate instantly forms, which is also rutile. Because high local concentration leads to quick and heterogeneous nucleation, primary nuclei of the precipitate are smaller and have more chance to coalesce. Simultaneously, NH_4Cl is produced as a by-product, which can have a detrimental effect. It was found that NH_4Cl would increase agglomeration among grains. Therefore, the hydrolysis has better porosity and bigger surface area.

$$TiCl_4 + NH_4OH \longrightarrow 4NH_4Cl + TiO_2 + H_2O$$

3.2 Experimental Results

We discuss results obtained from the different techniques like X-ray diffraction (XRD), Scanning electron microscopy (SEM), Fourier infrared spectroscopy (FTIR) and Transmission electron microscopy (TEM). The results are mainly divided in two parts:-

- Structural and morphological analysis, and
- Chemical analysis

Finally we have discussed the material physics behind the formation of such metal oxide complexes and the chemical and physical interaction between solvent and precursor used in the reaction.

3.2.1 Synthesis of TiO_2 prepared in acidic medium

- **XRD Analysis (Structural and morphological analysis)**

  In order to determine the size and to study the structural properties of the synthesized nanopowder of TiO_2, the powder XRD analysis was performed. From figure 3.1, it can be clearly observed that the diffraction peaks appear in the pattern corresponding to the mixed phase (anatase + rutile) with good crystalline nature. The diffraction peaks at $2\theta = 25.0^0$, 37.6^0, 53.7^0, 54.3^0, 62.4^0, 69.8^0 and 74.9^0 corresponds to the (101), (004), (200), (105), (211),

(204) and (215) planes of anatase TiO_2 (JCPDS No. 21-1272). Diffraction peaks were also observed at $2\theta = 26.9^0, 35.9^0, 43.7^0$. They were the (110), (101) and (210) diffraction peaks of rutile TiO_2 (JCPDS No.21-1276). The average particle size of TiO_2 nanoparticles has been calculated from full width at half maxima (FWHW) of the distinct peak (101) using Debye-Scherrer equation, and it is roughly estimated as 27 nm.

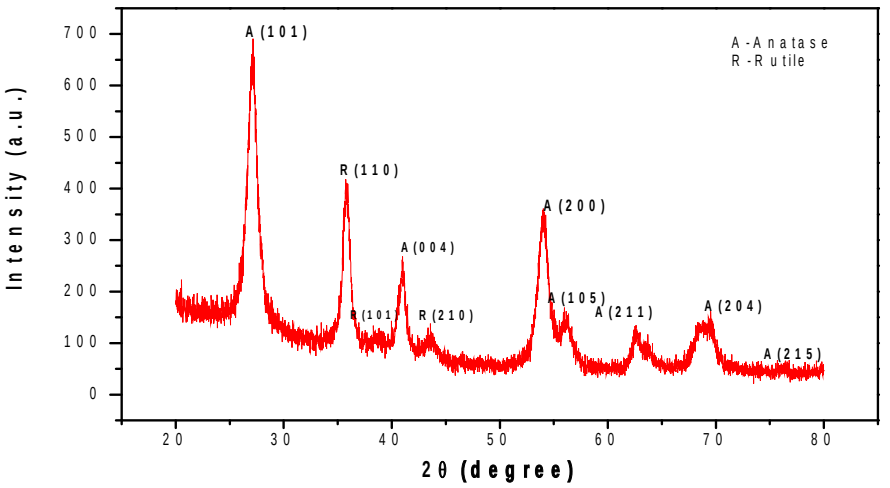

Figure 3.1 XRD spectra of synthesized TiO_2

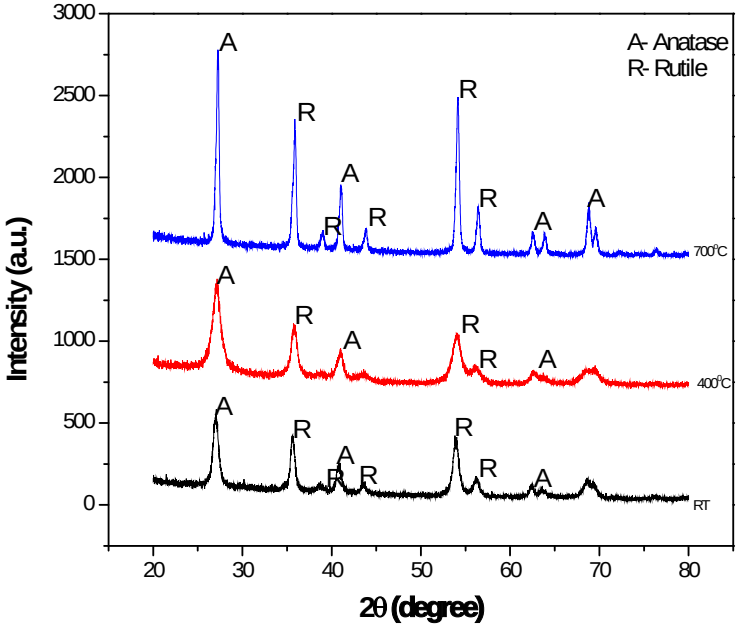

Fig 3.2 XRD spectra of calcined samples

In Figure 3.2, three samples were there in which two were calcined at different temperature for 4 hrs and the other was dried at room temperature. One of the sample was calcined at 400 ^{0}C and the other was calcined at 700 ^{0}C. It was found we were getting the mixed phase (anatase + rutile).The particle size using Debye Scherrer's formula is roughly estimated as 33 nm at 400^{0}C and 35 nm at 700 ^{0}C.

- **SEM micrographs (Structural and morphological analysis)**

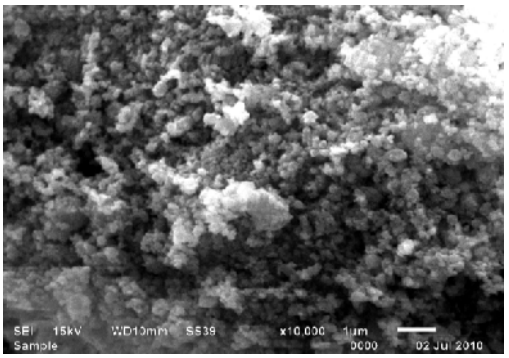

(a)

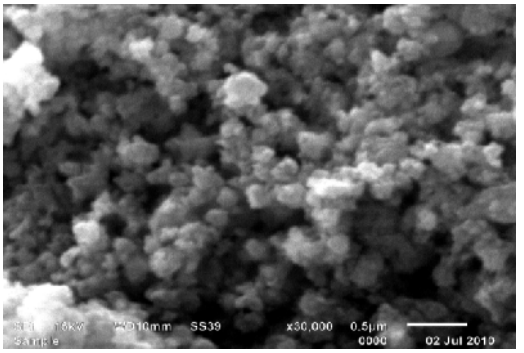

(b)

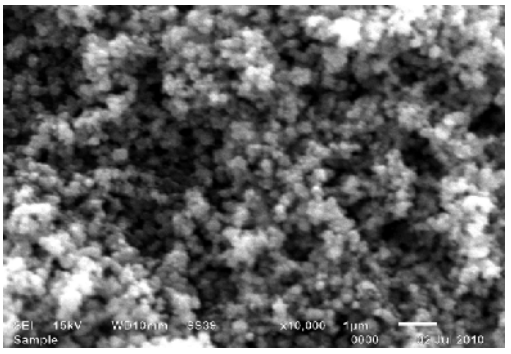

(c)

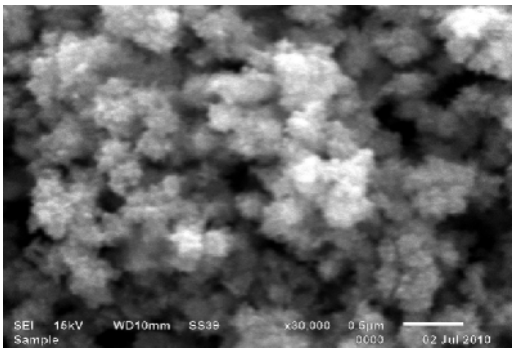

(d)

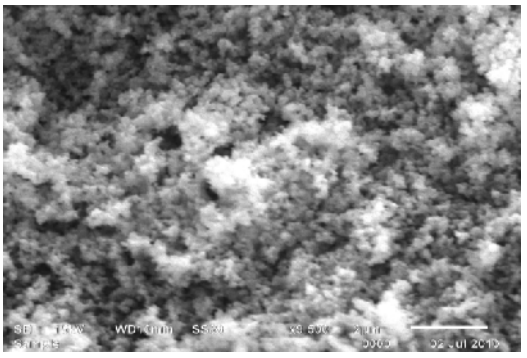

(e)

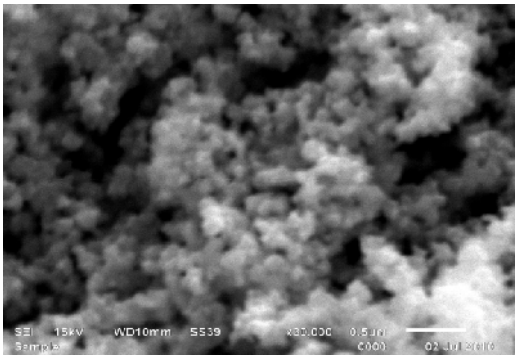

(f)

Fig 3.3 (a), (c), (e) SEM image at 10,000X & (b), (d), (f) SEM image at 30,000X

SEM micrographs of the synthesized TiO_2 nanoparticles are shown in figure 3.3.From the figure, it is quiet evident that there is no definite morphology in the sample. It seems that the particles were agglomerated and form clusters. Here, (a) & (b) were calcined at 400 ^{0}C for 4 hrs, (c) & (d) were dried at room temperature and (e) & (f) were calcined at 700 ^{0}C for 4 hrs. As the particle size calculated from the XRD is in nano range we are not getting any exact information about the surface morphology of the sample from the SEM micrograph, because of the limitation of our instrument. The morphology observed in the sample not showing any hard grains which gives the idea that size of the particle is small and further needs to be characterized by transmission electron microscopy (TEM) to obtained exact morphology and size of the particles.

- **FTIR Spectra of Synthesized TiO_2 (Chemical analysis)**

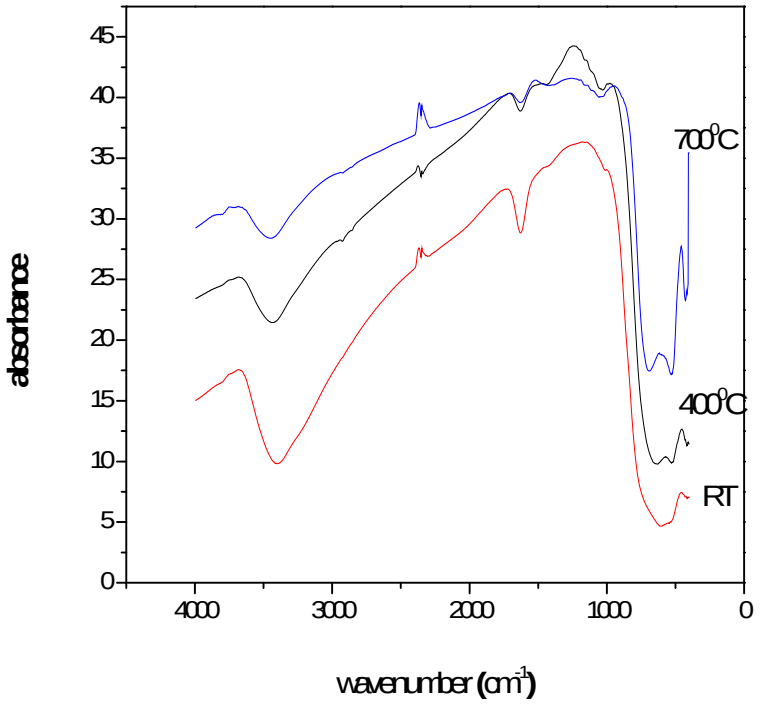

Fig 3.4 FTIR spectroscopy of synthesized TiO_2 nanoparticles

In figure 3.4 we were getting three peaks at different range. Bands observed in the 3350-3500 cm^{-1} range arise from the superposition of the ν_{OH} mode of interacting hydroxyl groups, the symmetric and antisymmetric ν_{OH} modes of molecular water coordinated to Ti^{4+} cations. The band at 1626 cm^{-1} was assigned to the molecular water bending mode, while the narrow bands at 534, 513 were due to the Ti-O-Ti.

Sample prepared at room temp. (cm^{-1})	Sample calcined at 400^0C (cm^{-1})	Sample calcined at 700^0C (cm^{-1})	Type of Bond
3398	3439	3460	H-O-H
1626	1626	1626	Molecular H_2O vib.
534	534	513	Ti-O-Ti

Table 3.1 Spectral interpretation of FTIR spectra

3.2.2 Synthesis of TiO_2 with ammonia (basic medium)

- **XRD Analysis (Structural and morphological analysis)**

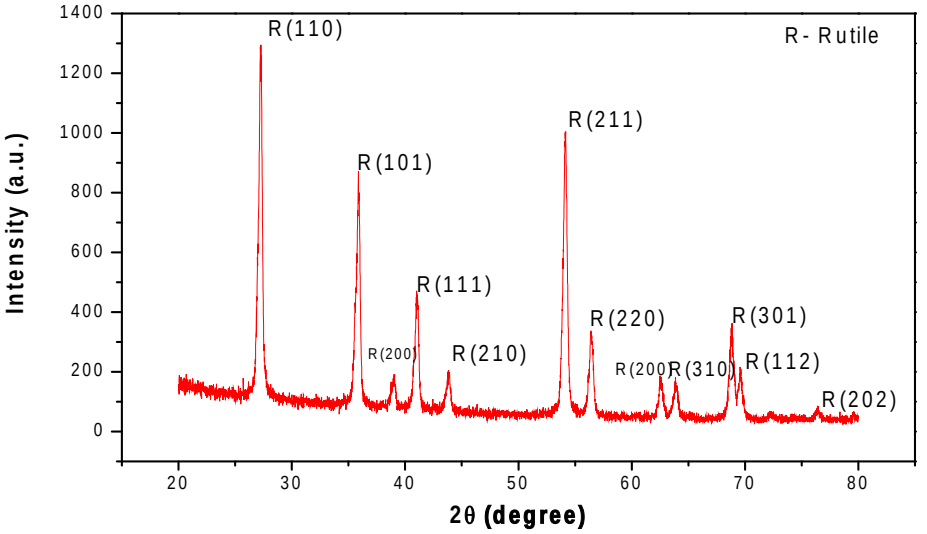

Fig 3.5 XRD spectra of synthesized TiO_2 with ammonia

Fig 3.5 shows the XRD pattern of the TiO_2 nanoparticles synthesized with ammonia. We observed that the sample is highly crystalline as evident from the XRD pattern in which broad peaks with high intensity extended over the 2θ scale. The peak observed at 2θ = 26.9^0, 35.7^0, 38.0^0, 40.8^0, 43.3^0, 53.7^0, 55.5^0, 62.6^0, 63.5^0, 68.4^0, 69.4^0 and 76.35^0 correspondence to the lattice plane (110), (101), (200), (111), (210), (211), (220), (002), (310), (301), (112) and (202) respectively. All the peaks are matched with standard JCPDS card no.(21-1276). The broadening of the peaks gives an idea about the small particle size of the synthesized TiO_2. Further, the

crystalline size D, corresponding to the (110) peak, was calculated by using the Scherrer's formula: $D=0.9\lambda/B\cos\theta$, where λ, B, θ are the wavelength, full width at half maxima (FWHM) and Bragg diffraction angle respectively. The calculated particle size was 30 nm.

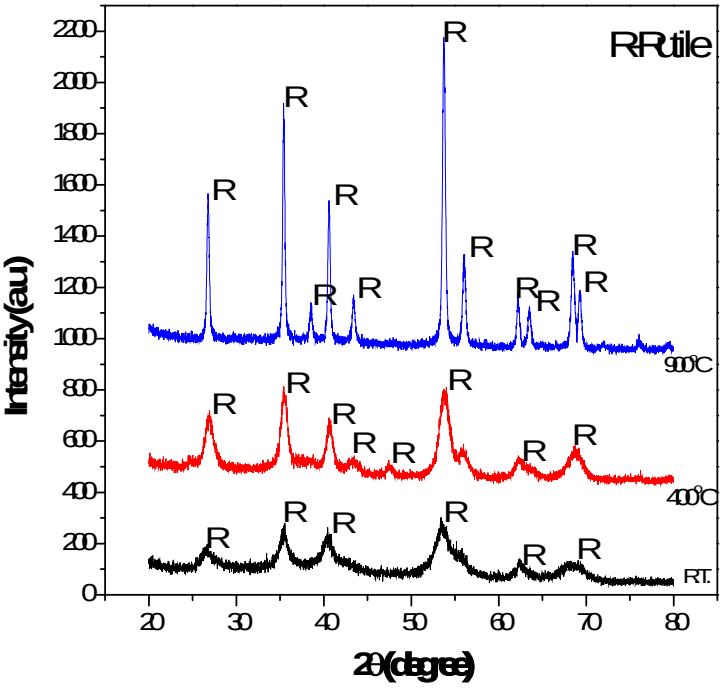

Fig 3.6 XRD spectra of calcined samples synthesized with ammonia

The XRD pattern of the synthesized TiO_2 in the presence of the ammonia are shown in the figure 3.6. Highly intense peaks observed in the XRD pattern indicated that all the samples are well crystalline. Out of the three samples, one is naturally dried in oven while the other two samples are calcined at different temperatures i.e. at 400 ^{0}C and 900 ^{0}C. It was observed that before calcination it has pure rutile phase and after calcination, it keeps rutile phase intact. From the above results we conclude that addition of ammonia makes the medium basic but do not disrupting the crystal structure of TiO_2. It gives the pure rutile phase. The particle size at 400 ^{0}C was 37 nm and at 900 ^{0}C was 39 nm.

- **SEM micrographs (Structural and morphological analysis)**

The SEM images of as prepared titania nanopowder with ammonia at the magnification of 10,000 and 30,000 as shown in figure 3.7. Here in this three samples were there in which (a) and (b)

were dried at room temperature, (c) and (d) were calcined at 400 ^{0}C for 4 hrs and (e) and (f) were at 900 ^{0}C for 4 hrs.

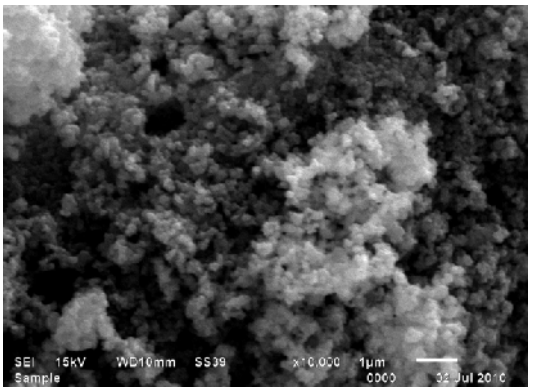

(a)

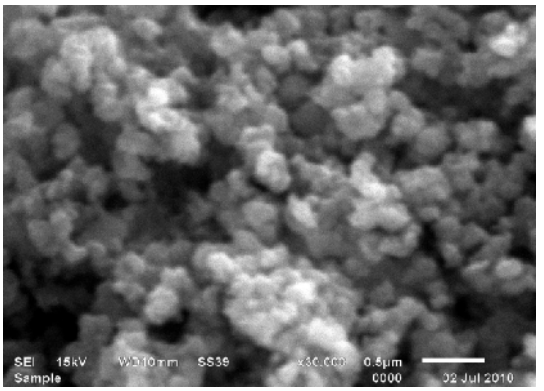

(b)

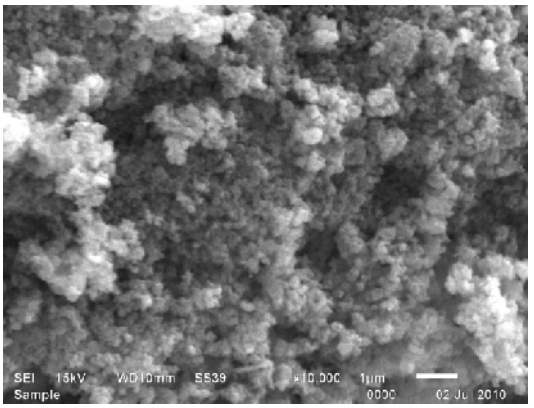

(c)

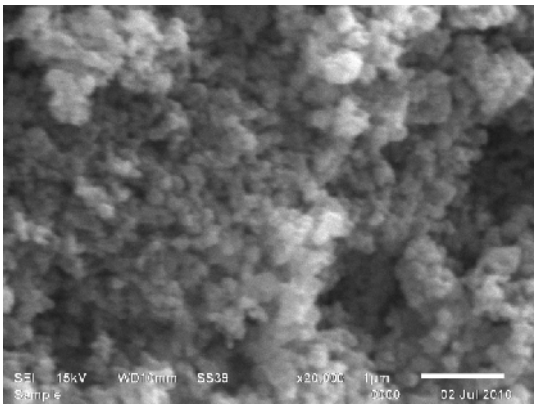

(d)

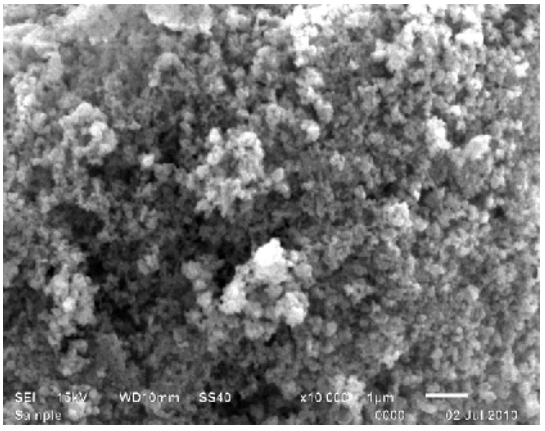

(e)

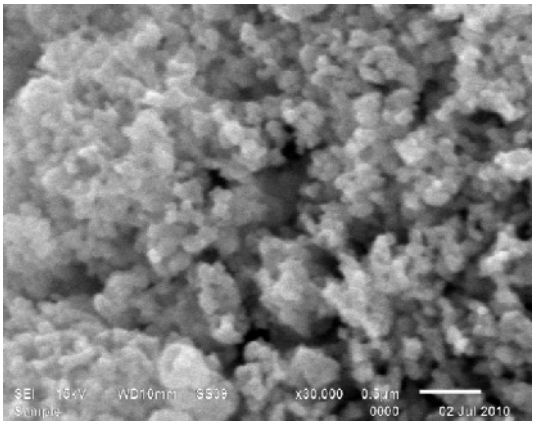

(f)

Fig 3.7 (a), (c), (e) SEM image at 10,000X & (b), (d), (f) SEM image at 30,000X

The formation of uneven spherical grains, which is a characteristic phenomenon of TiO_2 nanoparticles is observed in this work as well. The individual spherical particles are not clearly observed due to the formation of nanoclusters.

- **TEM analysis (Structural and morphological analysis)**

The transmission electron microscopy analysis was carried out to confirm the actual size of the particles, growth pattern and distribution of the crystallites. Rutile TiO_2 had acicular ellipse shapes as evidence from figure 3.8. They were 10-15 nm in width and 30-40 nm. Anisotropic crystal growth along the c-axis resulted in anisotropic acicular ellipse shapes of single crystals.

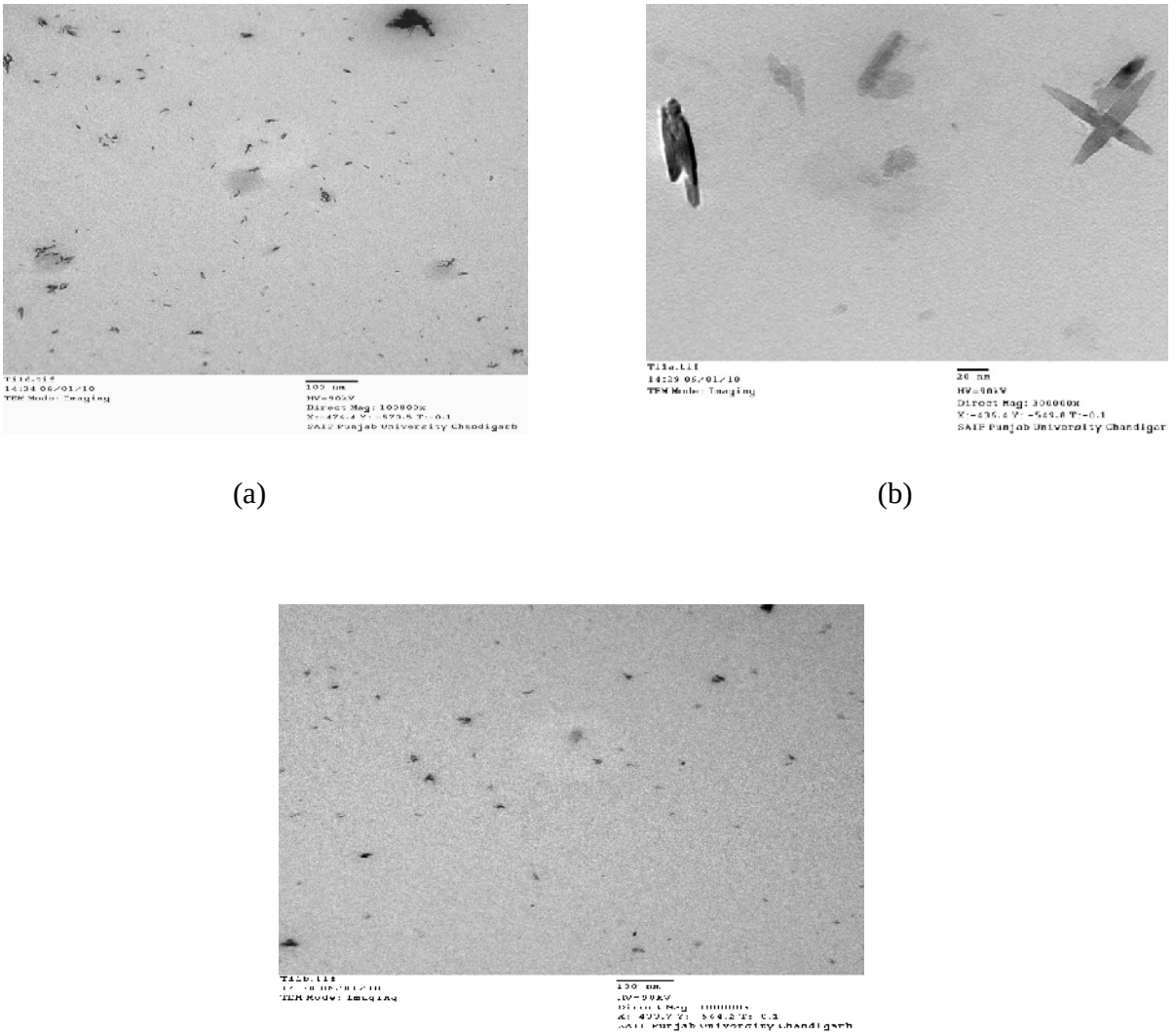

(a) (b)

(c)

Fig 3.8 TEM images of TiO_2 crystallites

- **FTIR spectroscopy (Chemical analysis)**

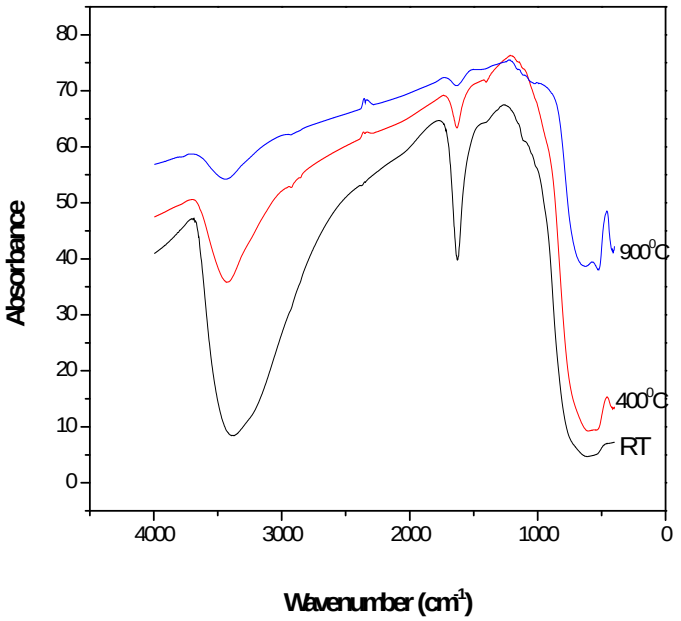

Figure 3.9 FTIR spectroscopy of synthesized TiO_2 nanoparticles with ammonia

Sample prepared at room temp. (cm^{-1})	Sample calcined at 400 ^{0}C (cm^{-1})	Sample calcined at 700 ^{0}C (cm^{-1})	Type of Bond
3370	3420	3437	H-O-H
1625	1625	1625	Molecular H_2O vib.
594	577	528	Ti-O-Ti

Table 3.2 Spectral interpretation of FTIR on adding ammonia

In figure 3.9 we were getting three peaks at different range. Bands observed in the 3350-3450 cm^{-1} range arise from the superposition of the ν_{OH} mode of interacting hydroxyl groups, the symmetric and antisymmetric ν_{OH} modes of molecular water coordinated to Ti^{4+} cations. The band at 1625 cm^{-1} was assigned to the molecular water bending mode, while the narrow bands at 534, 513 were because of the presence of the Ti-O-Ti.

CONCLUSIONS

TiO_2 nanoparticles are prepared by sol-gel technique by using easily available and cheap precursor of Ti i.e. $TiCl_4$. Effect of reaction pH on the structure of as-synthesized nanoparticles was investigated. It has been concluded that acidic reactions always gives mixed phase TiO_2 nanostructures i.e. (anatase+rutile), while basic reactions yields single phase rutile nanostructures. The effect of annealing on the structure and size of the nanoparticles was investigated by X-ray diffraction experiments. It was observed that the size of the nanostructures increases with annealing temperature irrespective of their structure. It was further concluded that the anatase phase diminishes as the annealing temperature increases. TEM pictures indicated that the nanostructures have rod-shaped morphology and they tend to agglomerate upon heating, which is evident from SEM images. Clean FT-IR spectra confirms that the nanostructures are free from any contamination.

REFERENCES

[1]. http://alanassad.com/sabbath/Elements/Ingorcanic/TiO2-Titanium%20Dioxide.pdf.

[2]. TiO_2 from Wikipedia, the free encyclopedia.

[3]. Goresy Chen, M Dubrovinsky, L Gillet, P Graup, Vol.293, 456-467 (2001).

[4]. http://www.azom.com/details.asp? Article ID=117.

[5]. Emsley, John, Nature's Building Blocks: An A-Z Guide to the Elements. Oxfords: Oxford University Press, Vol.56, 451-453 (2001).

[6]. Greenwood, Norman N, Chemistry of the Elements, Oxford Pergamon, Vol.67, 1117-1119 (1984).

[7]. "Titanium Oxide for High-Density Data Storage". Research, Vol.16, 567-577 (2010).

[8]. Lance G. Phillips, David M. Barbano, Journal of Dairy Science, Vol.80, 249-235 (2009).

[9]. Discovery and applications of photocatalysis, Vol.44, 987-994 (2005).

[10]. Fujishima, AKIRA, "Electrochemical Photolysis of Water at a Semiconductor Electrode". Nature, Vol. 238, 389-393 (1972).

[11]. Seung Yong Chai, Yong Joo Kim, Wan In Lee, Journal of Electroceramic, Vol.17, 909-912 (2006).

[12]. Jenny Hogan," Smog-busting paint soaks up noxious gases". Newscientist.com, Vol.24, 546-556 (2004).

[13]. Wu Le, Kan Su-Rong, Lu Shi-gang, Trans. Nonferrous Met. Soc., Vol.17, 789-791 (2007).

[14]. Jones BJ, Vergne BJ, Hayes, Anal. Chem., Vol.79, 423-428 (2007).

[15]. Lewis, Nathan,"Nanocrystalline TiO_2". Research, California Institute of Technology, Vol. 67, 478-485 (2009).

[16]. M. D. Earne,"Electrical Conductivity of TiO_2", Physical Review, Vol.61, 789-797 (1942).

[17]. Paschotta, Rudiger,"Encyclopedia of Laser Physics and Technology", RP Photonics, Vol.67, 567-579 (2009).

[18]. Sax, N.I. Richard,"Dangerous properties of Industrial Materials", Vol.3, 986-997 (2000).

[19]. "Titanium dioxide". International Agency for Research on Cancer, Vol.32, 167-179 (2006).

[20]. "Nano World: Nanoparticle toxicity tests". Physorg.com, Vol. 45, 1220-1227 (2006).

[21]. Kutal C, Serpone N, Photosensitive Metal Organic Systems: Mechanistic Principles and Applications. American Chemical Society, Vol.56, 2035-2047 (1993).

[22]. Yunhua Chen, An Lin, Funing Gun, Powder Technology, Vol.167, 109-116, (2006).

[23]. Chien-I Wu, Jiann-Wen Huang, Ya-Lan Wen, Shaw-Bing Wen, J. of Materials Letters, Vol.62, 1923-1936 (2008).

[24]. Zhang, Xiaoqiang; Yin, Lihong, Journal of Nanoscience and Technology, Vol.10, 5213-5217 (2010).

[25]. A. Ranga Rao and V. Dutta, Solar Energy Materials and Solar Cells, Vol.91, 1075-1080 (2007).

[26]. Yadong Yao, Yongdi Li, Wei Shao,Guangfu Yin, Journal of Wuhan Univ.Of Technology, Vol.24, 337-342 (2009).

[27]. Zhabo Wang, Guian Li, Honrui Peng, Zhikun Zhang, Journal of Materials Sciences, Vol. 40, 6433-6438 (2005).

[28]. Xu Wei-guo, Chen An-min, Zhang Qiang, Journal of Wuhan University of Technology-Mater.Sci.sd., Vol.19, 334-345 (2004).

[29]. Vilas S.Desai and Meenal Kowshik, Research Journal of Microbiology, Vol.4, 91-113 (2009).

[30]. Guifen Fu, Patricia S. Vary, Chhiu-Tsu.Lin, J.Phys. Chem. B, Vol.109, 8889-8898 (2005).

[31]. Huijun Zhang, Dajun Wu, IEEE International Conference on Nano/Micro engineered and Molecular Systems, Vol.45, 18-21 (2006).

[32]. Iram B. Ditta, Alex Steele, Howard a. Feoster, Appl. Microbial Biotechnol, Vol.79, 127-133 (2008).

[33]. S-Q Sun, B Sun, Wenqin Zhang and D Wang, Bull.Mater.Sci., Vol.31, 61-66 (2008).

[34]. Huanjun Zhang and Guohua Chen, Environ.Sci. Technol., Vol.43, 2906-2910 (2009).

[35]. San-Xiang Tan, Shaw-Zao Tan and Ding-Sheng Yuen, Sci. Technol. Adv. Matter., Vol. 10, 345-356 (2009).

[36]. Rahmani AR., Samar Ghandi Mr., Samadi MT., Nazemi F, J Res Health Sci, Vol.9, 3308 (2009).

[37]. Tiangyong Zhang, Huixian Shi, Quisheng Yang, Xu Liu, Cong Han, Journal of Physics: Conference Series, Vol.188, 2027-2038 (2009).

[38]. Shifu Chen, Sujuan Zhang, Wei Zhao, Wei Liu, J Nanopart. Res.,Vol.11, 931-938 (2009).

[39]. P. Hajkova, P. Spatenka, J. Krumeich and P. Koci, Eur. Phys. J. D, Vol.54, 189-193 (2009).

[40]. Beata Tryba, International Journal of Photo energy, Vol.72, 15-31 (2008).

[41]. E.D. Jeong, Pramod.H. Borse and H.G Kim, Journal of Ceramic Processing Research vol.9, 250-253 (2008).